Title

Radiologic evaluation of the kidney transplant donor and recipient

Authors

Goiffon, Reece J
Depetris, Jena
Dageforde, Leigh Anne
et al.

Publication Date

2024-07-10

DOI

10.1007/s00261-024-04477-4

Abdominal Radiology
https://doi.org/10.1007/s00261-024-04477-4

REVIEW

Radiologic evaluation of the kidney transplant donor and recipient

Reece J. Goiffon[1] · Jena Depetris[2] · Leigh Anne Dageforde[3] · Avinash Kambadakone[1]

Received: 10 May 2024 / Revised: 26 June 2024 / Accepted: 28 June 2024

Abstract

The kidney is the most common solid organ transplant globally and rates continue to climb, driven by the increasing prevalence of end stage renal disease (ESRD). Compounded by advancements in surgical techniques and immunosuppression leading to longer graft survival, radiologists evermore commonly evaluate kidney transplant patients and candidates, underscoring their role along the transplant process. Multiphase computed tomography (CT) with multiplanar and 3D reformatting is the primary method for evaluating renal donor candidates, detailing renal size, vascular/collecting system anatomy, and identifying significant pathologies such as renal vascular diseases and nephrolithiasis. Ultrasound is the preferred initial postoperative imaging modality for graft evaluation due to its low cost, accessibility, noninvasiveness, and lack of radiation. CT and magnetic resonance imaging (MRI) may be useful adjunctive imaging techniques in diagnosing transplant pathology when ultrasound alone is not diagnostic. Kidney transplant complications are categorized by an approximate timeline framework, aiding in differential diagnosis based on onset, duration, and severity and include perinephric fluid collections, graft compression, iatrogenic injuries, vascular compromise, graft rejection, and neoplastic processes. This review discusses imaging strategies and important findings along the transplant timeline, from donor assessment to long-term recipient complications.

Reece J. Goiffon and Jena Depetris have contributed equally to this work.

✉ Reece J. Goiffon
rgoiffon@mgh.harvard.edu

Jena Depetris
jdepetris@mednet.ucla.edu

Leigh Anne Dageforde
ldageforde@mgh.harvard.edu

Avinash Kambadakone
akambadakone@mgh.harvard.edu

[1] Department of Radiology, Massachusetts General Hospital, Harvard Medical School, 55 Fruit Street, White 270, Boston, MA 02114-2696, USA

[2] Department of Radiological Sciences, University of California Los Angeles Health, David Geffen School of Medicine at UCLA, 757 Westwood Plaza, Suite 1621, Los Angeles, CA 90095, USA

[3] Department of Surgery, Massachusetts General Hospital, Harvard Medical School, 55 Fruit Street, White 511, Boston, MA 02114-2696, USA

Published online: 10 July 2024

Graphical Abstract

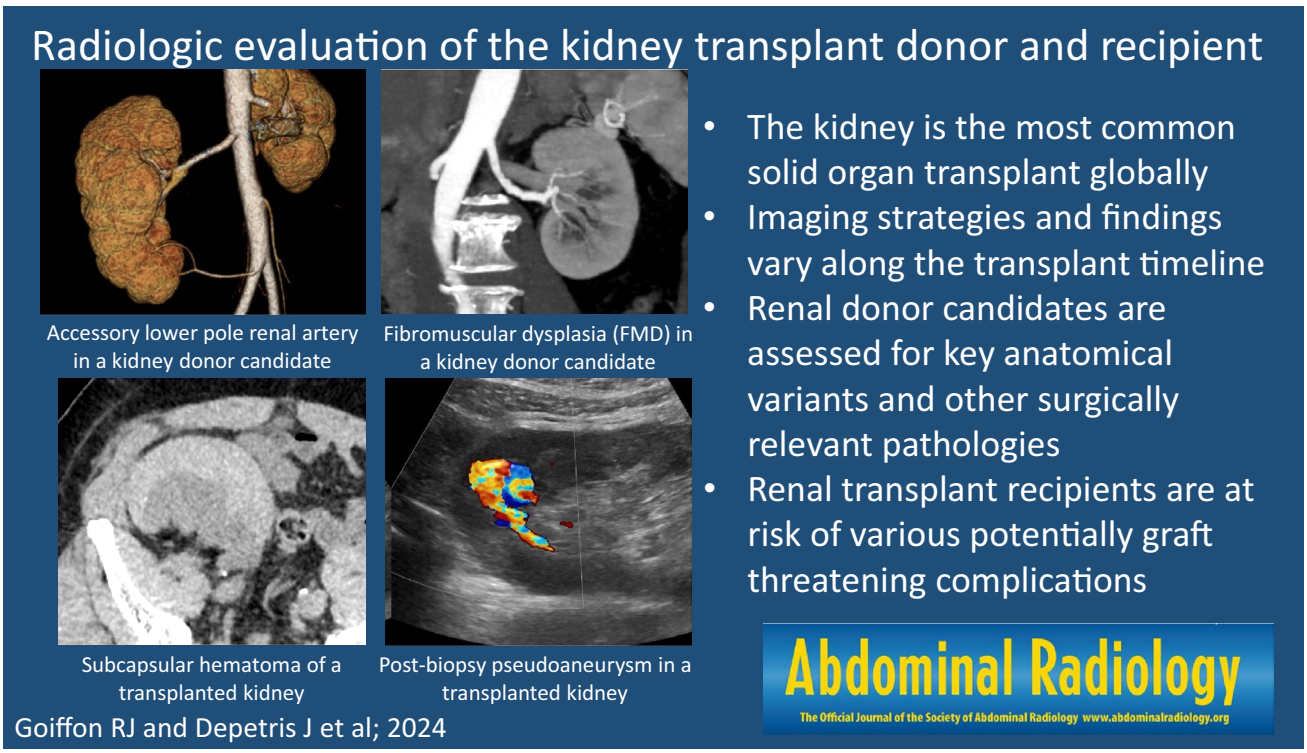

Keywords Renal donor · Kidney transplantation · Transplant complications

Abbreviations

CT	Computed tomography
CTA	Computed tomographic angiography
EMR	Electronic medical record
ESRD	End stage renal disease
FMD	Fibromuscular dysplasia
HU	Hounsfield unit
IVC	Inferior vena cava
MRI	Magnetic resonance imaging
MRA	Magnetic resonance angiography
MIPs	Maximum intensity projections
MPR	Multiplanar reconstruction
PSV	Peak systolic velocity
PACS	Picture archive and storage
PTLD	Post-transplant lymphoproliferative disorder
RACS	Renal allograft compartment syndrome
RI	Resistive index

Introduction

History and current state of kidney transplantation

The kidney was the first transplanted solid human organ and remains the most commonly transplanted today, driven by rising prevalence of end stage renal disease (ESRD) in the United States and globally (Fig. 1a) [1, 2]. Dialysis and kidney transplantation are the primary ESRD treatments. Although dialysis costs more than twice as much as transplantation with 5–6-fold increased mortality, dialysis is the primary therapy in the United States due to donor kidney scarcity (Fig. 1b) [2]. This shortage is somewhat alleviated by a steady rate of living kidney donation. Deceased donor kidney transplant rate has also increased over the past decade, partially due to young adult deaths from the opiate crisis and changes in donor and recipient eligibility criteria (Fig. 1c) [3]. As kidney transplant prevalence rises, so too does the need for radiologists' proficiency with kidney donor and recipient imaging.

Unlike deceased donors, who are explored surgically at organ harvest, living donor candidates are evaluated for key anatomy by radiologists, who also assess the post-transplant recipient for complications and help guide management by

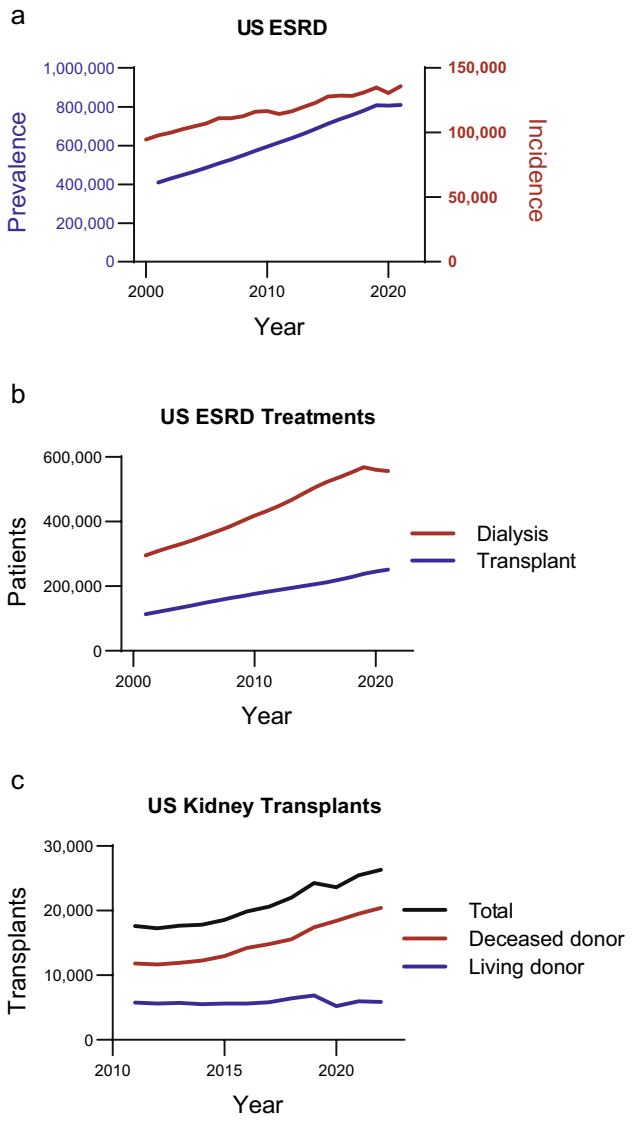

Fig. 1 Trends of ESRD in the United States. **a** Increasing incidence and prevalence of ESRD since 2001. **b** Prevalence of ESRD treatment modalities among living patients. **c** Rate of kidney transplants by donor type. Adapted from [2, 3]

the transplant team. This review covers imaging strategies and findings throughout the transplant timeline, from donor evaluation to chronic recipient complications.

Imaging techniques for the kidney donor

Computed tomography

Multiphase computed tomography (CT) is less invasive and more accurate than intravenous pyelography and angiography used historically to evaluate the kidneys, renal vasculature, and collecting systems. Donor evaluation requires at least two contrast phases: arterial phase for assessing the renal cortical volume and arteries, and excretory phase for the ureters and parenchymal lesions. Arterial phase can be accomplished with injection timing or bolus tracking per institutional preference [4, 5].

Additional contrast phases and reconstructions vary by practice [4–8]. Stone detection can be performed on non-contrast acquisition, arterial and nephrogenic phases, or virtual non-contrast images from dual energy/spectral acquisitions which reduce radiation while maintaining at least 90% sensitivity [9]. Nephrogenic phase may help delineate the renal veins and increase sensitivity for renal and extrarenal pathology. Excretory phase images are either conventional CT stacks or a repeat topogram, which is sufficient for gross ureteral anatomy. Nephrogenic or delayed phase images may extend into the pelvis or be limited to the upper abdomen to reduce radiation. The protocol used at one of the authors' institutions is described in Table 1.

Multiplanar and 3D reconstruction

Modern helical, multidetector CT data can create volumetric, thin-slice images to allow for multiplanar reconstruction (MPR) by the interpreting radiologist on the picture archive and storage (PACS) system. While this obviates the need for separate coronal and sagittal images for the radiologist, 3 mm thick coronal and sagittal images are still usually sent to PACS for viewing in the electronic medical record (EMR) by the transplant team. These thicker coronal and sagittal images are not adequate to detect subtle but important findings such as vasculopathies, ostial calcifications, and small renal stones due to the Nyquist sampling theorem.

3D images created by a technologist are useful to referring clinicians without PACS access to help conceptualize the spatial relationships between the anatomic structures. These can include curvilinear planes following key vessels, maximum intensity projections (MIPs) showing single-image vascular relationships, and 3D rendered rotating anatomic models. The choice of images sent to the EMR must be made in context of referring transplant team's expectations as well as 3D technologist availability or, without this resource, the time and technology constraints of the radiologist.

Magnetic resonance imaging

Magnetic resonance imaging (MRI) is an alternative for donor evaluation, offering advantages like the absence of ionizing radiation to typically young and healthy donors, no risk of contrast-induced nephropathy, lower risk of allergic-like contrast reactions, and better characterization of incidental lesions. Studies suggest lower test performance metrics with contrast-enhanced magnetic resonance angiography (MRA)

Table 1 Example of a kidney donor evaluation CT protocol

Contrast	Oral: water Intravenous: 370 mg/mL iodine, mixed and injected by patient weight 50 mL, 75% contrast + 25% saline, 3.5 mL/s (under 250 lb) 80 mL, 100% contrast, 4 mL/s (over 250 lb) 40 mL saline, 4 mL/s after contrast (all weights)
Acquisitions	1. Topogram 2. (If single energy CT) precontrast, left atrium to iliac arteries 3. Postcontrast bolus tracking series, upper abdominal aorta, 150 HU trigger with 10 s diagnostic delay 4. Arterial phase, left atrium to iliac arteries 5. Topogram (6 min) 6. Delay phase (6 min), left atrium to iliac arteries
Reconstructions	1. (If single energy CT) precontrast 2 mm thick and spacing in transaxial, coronal, and sagittal planes 2. (If dual energy CT) arterial phase: (a) 50 kEv, 1.25 mm thick, 0.625 mm spacing (b) virtual noncontrast, 2.5 mm thickness and spacing, (c) iodine maps 2.5 mm thickness and spacing 3. (If single energy CT) atrial phase: 1.25 mm thick, 0.625 mm spacing 4. 6 min delay: 5 mm thickness and spacing 5. Coronal and sagittal: arterial phase, 3 mm thickness and spacing (archival) 6. 3D lab cortical volumes 7. 3D lab batch oblique coronals through right and left renal hila (archival) 8. 3D lab MIP single images (minimum 4) of renal arteries, renal veins (archival)
Other	Radiologist saves archival images of each measurement and curvilinear vessel reconstructions, if performed

compared to CT angiography (CTA), especially in detecting arterial variants [10–12]. Image quality depends on field strength: 3 Tesla magnets can produce higher-quality images while underestimating arterial diameter, overestimating renal artery stenosis, and potentially suffering from medical hardware-induced artifacts in some patients [13].

Nuclear renal scintigraphy

Renal scintigraphy was the first widely used modality for quantifying split renal function [14]. More recently, cortical volume measurement by CT has demonstrated high correlation with scintigraphy [15, 16], thus CT has supplanted routine scintigraphy in many transplant centers. Nuclear studies may still be used to delineate split function if there is > 10% volume discrepancy on CT. At one author's institution, this is typically performed by injecting 370 MBq (10 mCi) ^{99m}Tc-mercapto acetyl triglycine (MAG3) and measuring peak renal uptake over 30 min. If split function discrepancy > 10% is confirmed, the smaller kidney is still considered based on intended recipient size. If it is too small, the donor can still donate to a smaller-bodied recipient as part of a paired- or chained-donor arrangement, thus allowing the originally intended recipient to receive a different, larger kidney.

Assessing the renal donor

Living donor surgical approaches

Understanding the surgical approach for donor nephrectomy helps the radiologist distill pertinent anatomic details on CT. Nearly all nephrectomies (> 98%) are performed using minimally invasive techniques including pure laparoscopic, hand-assisted laparoscopic, and robot-assisted techniques through either a transperitoneal or retroperitoneal approach [3] (Fig. 2a). Hand-assisted laparoscopic nephrectomy is the most common approach and may have lower complication rates but longer hospital stays compared to robot-assisted nephrectomy [17, 18]. All three techniques may utilize an anterior approach through a low midline, transverse suprapubic, or ipsilateral incisions for gel, camera, and instrument ports [17]. Left nephrectomy is preferred as the left renal vein is usually longer, making for easier implantation. In an anterior approach left nephrectomy, the left colon, spleen, and pancreatic tail are medialized to expose the renal fossa, while on the right, the liver is retracted and the right colon and duodenum are medialized. The retroperitoneal approach provides a more direct route to the kidney but can be less accessible due to trans-muscular route and a tighter working space, possibly limiting harvestable renal vessel length [19].

Renal and vascular measurements

Renal length should be measured using MPR images aligned to the principal and secondary orthogonal long axes, given that kidneys often lie obliquely, making coronal measurements unreliable [20] (Fig. 2b). Kidney length is a poor predictor of renal function [21, 22], so parenchymal or cortical volumes should also be reported—both are valid as proxies for renal function [23]—as assessed by the radiologist, a 3D technologist, or automated segmentation software. These volumes

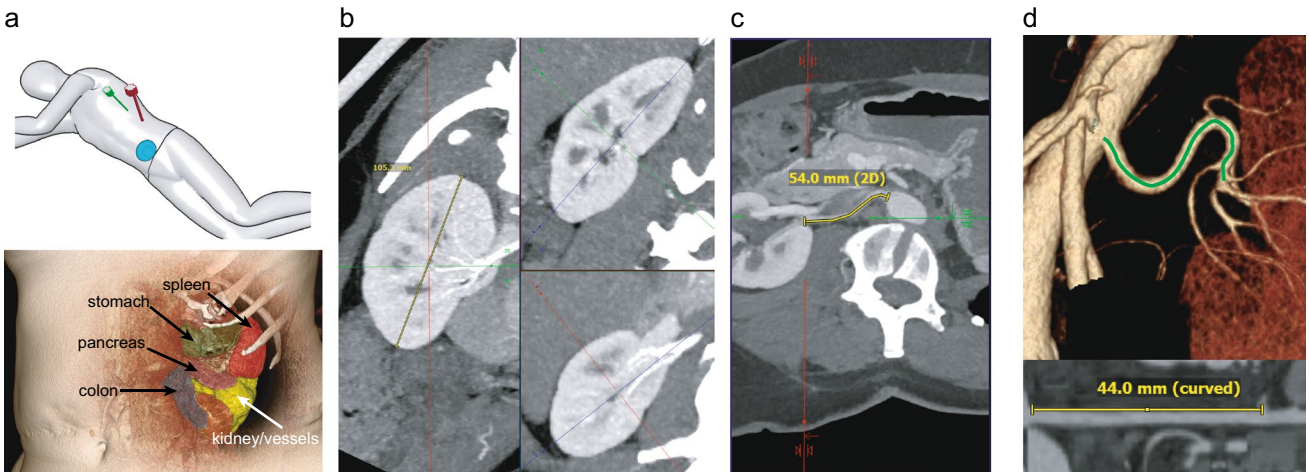

Fig. 2 Renal donor surgical and measurement techniques. **a** (above) Surgical approach of hand-assisted laparoscopic donor nephrectomy with suprapubic gel port (light blue) and camera/manipulation ports (green and red). (below) 3D CT reconstruction showing anterolateral view from a camera port angle with the kidney/renal vessels (yellow, white arrow) partially obscured by viscera, requiring retraction. **b** Double-oblique MPR technique for measuring true renal length. **c** single plane curved measurement of a renal artery. **d** centerline curvilinear measurement of a tortuous renal artery

are used to estimate split function for triaging which kidney to donate, as current published data are too preliminary to support an absolute renal volume cutoff for transplantation [24–26].

The simplest method for measuring straight or short vessels involves aligning an MPR axis along the vessel length and taking a linear measurement. Curved vessel segments contained within a single plane can be measured using multiple segments or curved measurement tools found in many PACS toolsets. Slight deviations from a double oblique plane (within a vessel diameter) can be "flattened" using MIPs with minimal loss of accuracy (Fig. 2c). More tortuous vessel segments may require curved plane reconstruction or vessel centerline segmentation, either native in PACS or with dedicated 3D software (Fig. 2d).

Vascular measurements are tailored to the surgical approach and structures that may limit access to the renal vessels. The hilar arteries are measured from the aorta to the first segmental branch or until they enter the renal sinus, noting any earlier branching polar or capsular arteries (Fig. 3a).

The right renal vein length is determined from the union of its last segmental tributaries to the inferior vena cava (IVC). The left renal vein is measured four times: from each of two upstream points (the last segmental junction and the insertion of the left gonadal vein) to each of two points downstream (the IVC and the left aorta margin) (Fig. 3a). These measurements aid in planning both anterior and retroperitoneal surgical approaches.

Vascular anatomy and variants

Renal arteries are classified as hilar, entering the renal sinus to perfuse the kidney centrifugally, or polar, traversing the capsular cortex to perfuse centripetally (Fig. 3b). One to three renal arteries are typical, the largest defined as the main renal artery and smaller arteries as accessory regardless of their perfusion distribution. Early segmental branching is a variant with the first left renal artery segmental branch within 1 cm of the aorta or the right branch within 1 cm of the right IVC margin, which may require special surgical consideration. Retrocaval branching of the right renal artery should also be reported, as this limits renal artery manipulation from anterior approach (Fig. 3c).

Small upper polar arteries, especially smaller than 3 mm, may be sacrificed during transplant, but lower polar and hilar arteries are preserved to prevent ischemic ureteral necrosis, necessitating detailed description of lower pole accessory arteries including diameter (Fig. 3d). Lower polar arteries can arise from the distal aorta or, rarely, the iliac arteries (Fig. 3e). Also rarely, a precaval accessory artery can congenitally enlarge to become a main pre-caval right renal artery, decreasing retroperitoneal accessibility (Fig. 3f). Smaller capsular arteries, branching from renal arteries or the aorta and perfusing the capsule and adjacent tissues, are generally not preserved during transplant but must be accurately identified to avoid confusion with polar arteries.

The renal veins are more variable than the renal arteries due to their embryologic origin as bridges between the ventral (subcardinal) and dorsal (supracardinal) venous

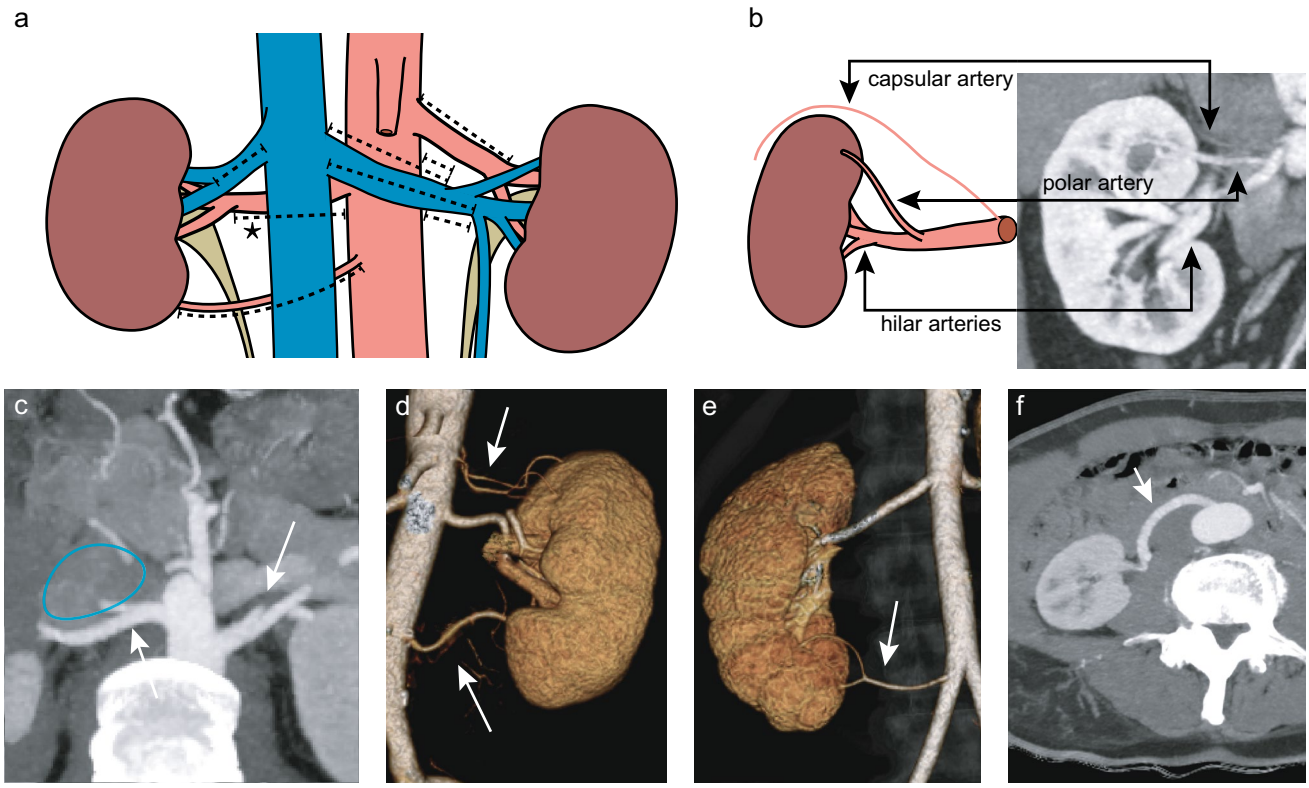

Fig. 3 Normal and variant vascular anatomy. **a** Arterial measurements from the aorta to first segmental branches, including a measurement from the right IVC margin (*) if there is < 1 cm early segmental branching. Venous measurements from the IVC to last segmental tributaries, IVC to left gonadal vein, and the same left landmarks to the left aortic wall. **b** Hilar, polar, and capsular artery diagram mirroring an example from a renal donor CT. Any of these can arise from the main renal artery or directly from the aorta. **c** Olique transaxial CT of bilateral early arterial segmental branching, with a retrocaval variant on the right, the inferior vena cava countour shown in blue. **d** 3D volume rendering of left upper and lower polar arteries arising from the aorta, the lower pole artery important for ureteral perfusion. **e** 3D volume rendering of a right lower pole artery arising from the common iliac artery. **f** Precaval main right renal artery, important if retroperitoneal approach is a surgical consideration

systems [27]. The right renal vein typically forms from this ventral-dorsal anastomosis, leading to duplicated veins in about 1 in 6 patients [28]. The left renal vein originates from a collar of three venous bridges around the aorta: the intersubcardinal, intersupracardinal, and sub-supracardinal anastomoses. During normal development, the supracardinal anastomosis regresses, leaving the pre-aortic left renal vein composed of the remaining two anastomoses. A circumaortic vein results if both intercardinal anastomoses persist, while a retroaortic vein forms if only the intersubcardinal anastomosis regresses. Any retroaortic component often communicates extensively with the lumbar/azygos system, also of supracardinal origin (Fig. 4a). The retroaortic vein can also insert low on the IVC or left iliac vein (Fig. 4b). These variants are well-reported, each occurring in about 1 in 30 patients. If circumaortic, the diameters and lengths of each component should be reported, as should any lumbar plexus bridging veins > 5 mm in diameter that increase risk of hemorrhage. Other venous variations such as duplicated, left, or absent IVC should also be described in detail with renal vein length measured to the first downstream central vein (Fig. 4c).

Renal vascular diseases

Atherosclerosis, the most common vascular disease in living renal donors, is increasingly common as donors over 55 years old have risen from 1 in 6 donors to 1 in 4 since 2011 [3]. Mild atherosclerosis does not preclude donation, but the more affected vessel is typically transplanted to reduce donor risk. An exception is made for coarse ostial calcification, which can complicate vessel closure during harvest, potentially causing hemorrhage or intimal laceration leading to thromboembolism (Fig. 5a). While there are no definitive criteria for donor eligibility based on vessel condition, radiologists should document the area percentage of cross-sectional narrowing at significant stenoses and measure the proximity of major calcifications to the arterial ostium.

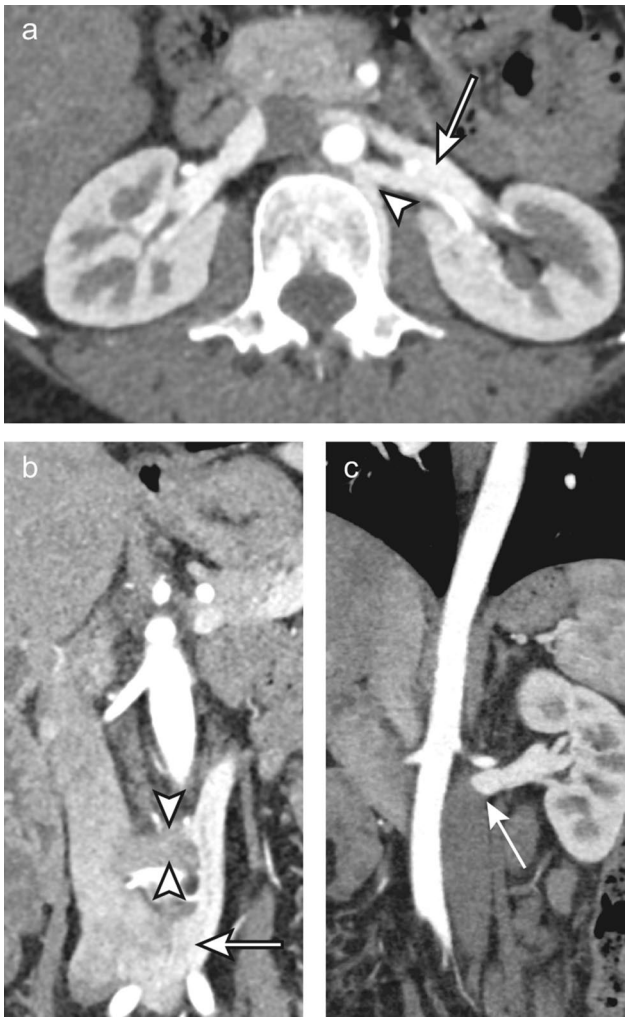

Fig. 4 Renal vein variants. **a** Circumaortic left renal vein with equal pre- and retroaortic veins, a preserved sub-supracardinal anastomosis near the renal hilum (arrow), and a prominent retroaortic-lumbar communication (arrowhead). **b** A low retroaortic left renal vein inserting on the left common iliac vein (arrow) and via a large lumbar-IVC plexus vein (arrowheads). **c** A left renal vein inserting on a left IVC with empty retroperitoneal fat to the right of the infrarenal aorta

Fibromuscular dysplasia (FMD) is a non-inflammatory vasculopathy affecting medium to large vessels, predominantly diagnosed in middle-aged females, and most commonly involving the renal arteries [29]. This condition can lead to dissections, aneurysms, and stenosis and is likely underdiagnosed due to its imaging similarities with atherosclerosis and its tendency to be asymptomatic [30]. On CT, FMD can present as beading from alternating strictures and aneurysms, long smooth stenoses from thrombosed dissections, or fenestrated dissection flaps [31] (Fig. 5b). Mild FMD may be challenging to detect on CT [32] and can progress post-transplant to disease threatening renal function, making it a conundrum when approving renal donors [33, 34].

Despite FMD's association with progressive renal insufficiency, data from FMD-positive donors show no significant long-term risks post-donation, likely in part due to selection bias for only mild cases approved for donation [35]. As incidental FMD in potential donors typically lacks symptoms and prior imaging, further assessment by a vascular specialist is crucial to manage the elevated risks of renal hypertension, stroke, and peripheral vascular disease associated with FMD and similar vasculopathies regardless of if the donor is committee-approved for surgery. Imaging appearances of FMD and inflammatory vasculitides such as polyarteritis nodosa can overlap but differ greatly by treatment, further emphasizing the need for specialist referral to further evaluate the vascular abnormality.

Collecting system variants

Small cadaveric studies have reported partial ureteral duplication in 2–5% of surveyed kidneys [36] and a larger study of candidate kidney donors showed single bilateral ureters in > 98% of patients [37]. While ureteral duplication does not disqualify a donor, surgeons must be aware of the duplication to avoid damaging the common circulation and causing ischemic necrosis. With modern techniques, duplicated ureters are not linked to a higher risk of ureteral complications [38], although the surgeon may instead take the other kidney if there are no contraindications (Fig. 5c).

Nephrolithiasis

Historically, renal stones were often a contraindication for donation. Today, after recognizing that about 8% of asymptomatic adults have stones, most stones being small and few in number, and data show comparable graft survival rates in stone-bearing allografts, transplant teams are now less apprehensive of donor stones [39–41]. With a history of stones or stones on pre-donation CT, a potential donor may undergo 24 h urine collection analysis to assess the stone etiology and risk of future stones. In cases of unilateral cortical stones < 5 mm, the affected kidney is preferentially donated and a ureteral stent is left in place post-transplant. Larger stones may be treated post-nephrectomy through ex vivo methods like back table pyelotomy, ureteroscopy, and lithotripsy before graft implantation [42]. Stones > 5 mm may increase risk of recipient complications (Fig. 5d, e).

Calcified renal stones can be detected on non-enhanced, virtual non-enhanced dual-energy, or contrast-enhanced images depending on institutional preference. The location, number, and size of stones should be reported based on measurements using bone window/levels to prevent blooming artifact from inflating stone size. If cortical stones

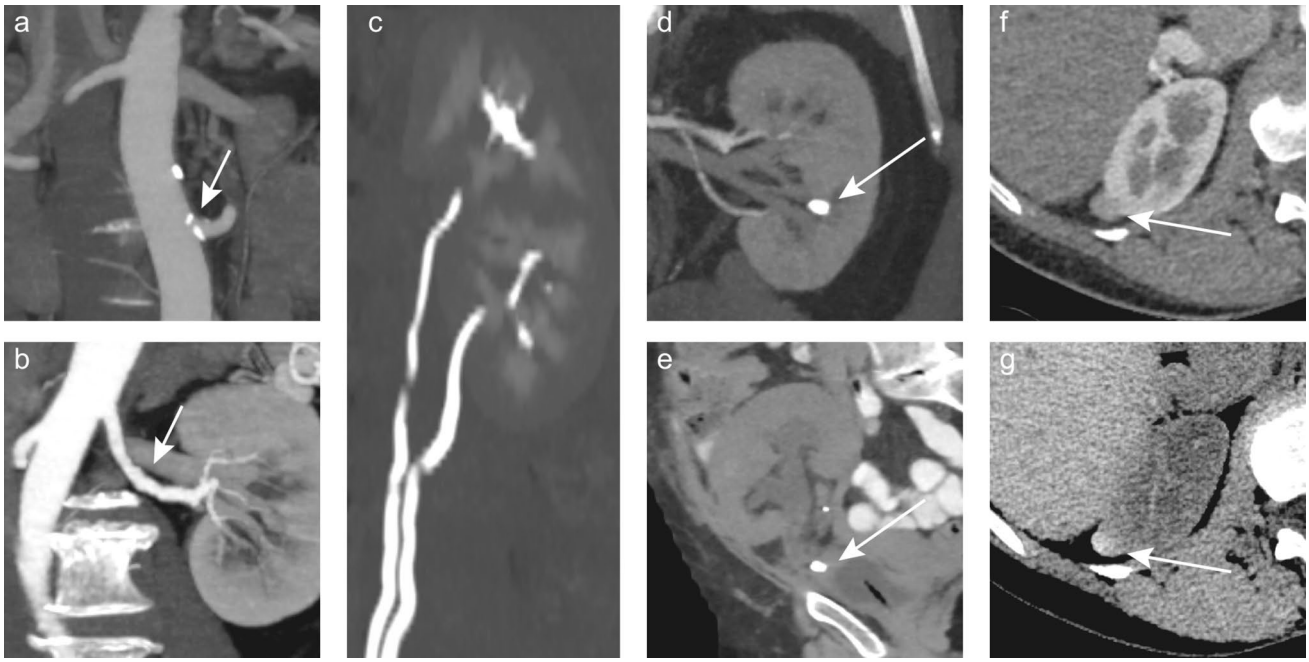

Fig. 5 Significant donor abnormalities. **a** Ostial atherosclerosis in a low main left renal artery. The patient was declined as a donor due to renal artery atherosclerosis. **b** Fibromuscular dysplasia with mid renal artery beading. The patient was declined as a donor due to severity and multifocality of FMD lesions. **c** Duplicated left ureters. The right kidney with normal vessels and a single ureter was instead donated. **d** A 7 mm stone in the candidate donor kidney. The right kidney was not donated due to vascular anatomy. **e** The same stone 5 months later in the recipient, now migrated into and obstructing the ureter. **f** An indeterminate lesion, possibly a mass on arterial phase. **g** Virtual nonenhanced image from the CT showing intrinsic hyper attenuation in keeping with a proteinaceous cyst, later confirmed on MRI

are present, the ureters and bladder (if imaged) warrant extra scrutiny to exclude stone migration into the collecting system.

Renal lesions

Transplanting kidneys with small suspected renal tumors, including renal cell carcinoma, is a viable strategy to expand the donor pool to help meet the growing need for kidney transplants [43]. Studies show that the risk conveyed by possible cancer recurrence in recipients of kidneys with renal cell carcinoma is very low, particularly when compared to the risks of remaining on hemodialysis [44]. Renal masses, large cysts, and benign mixed solid-cystic lesions can be removed via partial nephrectomy on the back table prior to transplantation depending on lesion size and location as well as other donor and recipient characteristics.

Multiphasic CT for donor evaluation provides a non-enhanced, arterially enhanced, and variably a nephrogenic and/or excretory phase set of images for enhancement assessment, increasing specificity compared to routine monophasic CT (Fig. 5f, g). While MRI can further characterize indeterminate renal lesion contents, it is not commonly employed due to the low risks associated with transplanting kidneys after back-table mass excision. Further diagnostic workup should be pursued if the patient is not approved for donation to minimize their own future risk.

Imaging techniques for the transplant recipient

Ultrasound imaging protocol

Ultrasound is the preferred initial imaging modality for evaluating renal grafts due to low cost, accessibility, noninvasiveness, and lack of radiation, which is crucial given the frequent and long-term monitoring needed for transplant recipients. It is used both routinely to establish a postoperative baseline and as needed for diagnosing complications. Examinations should be performed with a linear transducer, frequency range 2–18 MHz, and ideally with the patient well-hydrated. Standard protocol includes grayscale and color Doppler imaging of the graft and urinary bladder.

Grayscale assessment of the graft evaluates for size, parenchymal echotexture, hydronephrosis, and perinephric collections. Color Doppler assesses global graft perfusion and patency of the graft vasculature, including renal vein, renal artery at the hilum, mid-artery, and anastomosis, and

interlobar arteries at the polar and interpolar regions. The renal vein should show continuous flow with respiratory variability. The renal artery and interlobar arteries should exhibit a waveform with rapid systolic upstroke and continuous, anterograde diastolic flow. The renal artery resistive index (RI) quantifies distal resistance, calculated as (peak systolic velocity – end diastolic velocity)/peak systolic velocity, with normal values of 0.50–0.70. Finally, urinary bladder evaluation should document bladder distention, ureteral stent location (common postoperatively), a ureteral jet, and any filling defects.

Magnetic resonance and computed tomography considerations

CT and MRI are less commonly used in kidney transplant evaluation in part due to radiation and contrast induced nephropathy with CT and length of exam time and poor spatial resolution with MRI. However, both can be adjunctive techniques, providing extra diagnostic information after initial ultrasound evaluation if needed.

For example, if ultrasound cannot clearly assess graft vasculature due to bowel gas shadowing or poor sound penetration, CTA or MRA can measure vessel patency. CT protocols can be custom tailored to minimize risk of contrast-induced nephropathy. CT and MRI offer 3D reformatting capabilities and enable more comprehensive graft and surrounding anatomic evaluation, for example when assessing deep perinephric fluid collections. CT and MRI urography can also help localize urinary leaks, which is difficult with ultrasound.

Post-transplant complications

Complication timeline

Kidney transplantation can involve various complications such as iatrogenic injuries, vascular compromise, urinary issues, perinephric fluid collections, graft rejection, and infectious or neoplastic processes, many of which will be discussed later. Kidney transplant complications can be categorized by postoperative timing into early (including hyperacute and acute), intermediate, and late stages [45] (Fig. 6). Although complications may vary in onset timing, duration, and severity, this timeline framework helps narrow the differential diagnosis in evaluating kidney transplant pathology.

Perinephric collections

Perinephric collections are common posttransplant complications with typical postoperative timeline occurrence windows, from earliest to latest: hematoma, urinoma, abscess, and lymphocele. Although imaging features may overlap, correlating clinical factors with color Doppler ultrasound and adjunctive CT or MRI can confirm the diagnosis.

Perinephric hematomas typically occur from minutes to 5 days post-transplantation [45] but can occur anytime due to the graft's vulnerable anterior pelvic position. Perinephric hematomas appear on grayscale ultrasound as complex collections with heterogeneous echotexture and possible internal septations or retractile clot (Fig. 7a) without internal vascularity on color Doppler. Noncontrast CT shows hyperattenuating blood products > 30 HU (Fig. 7b), and

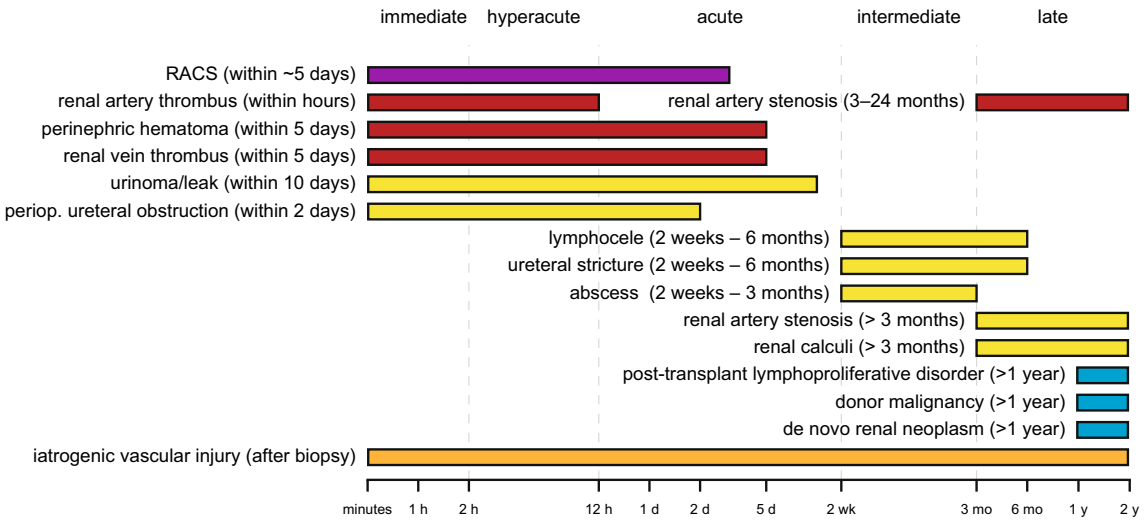

Fig. 6 Approximate timeline of post-transplant complications assessed by imaging. Adapted from [45]

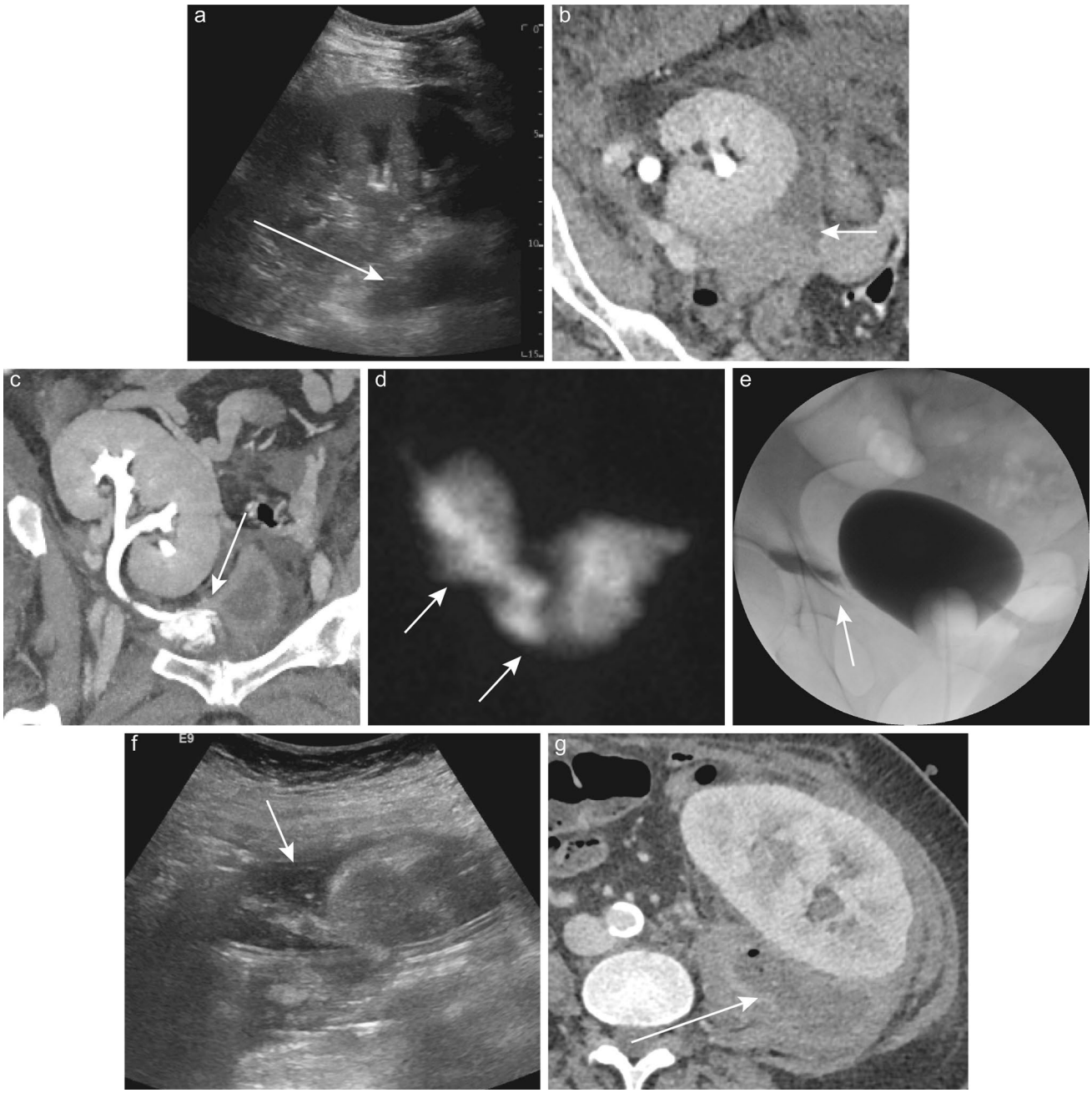

Fig. 7 Imaging of perinephric collections. **a** Ultrasound of a collection (arrow) along the renal hilum 2 days after transplant and **b** CT the following day showing a hematocrit level (arrow) indicating a hematoma. **c** Delayed phase CT 3 days after transplant showing extravasation at the ureteral anastomosis. **d** Renal scintigraphy and **e** cystogram performed on a different patient on post-transplant day 6 confirming an active urine leak (arrows). **f** Ultrasound 1 month after transplant showing a heterogenous collection, followed by **g** CT at 4 months showing organization of the collection into an abscess

multiphasic CTA may be used to find active bleeding sources in expanding hematomas. Most perinephric hematomas resolve spontaneously, though some require treatment if they significantly compress the graft, as discussed below.

Perinephric urinomas are collections of urine leaking from the renal collecting system, typically from the renal pelvis, ureter, or ureteral anastomosis. This complication often occurs within 10 days of transplantation, due to inadequate blood supply to the ureter, urinary tract pressures from obstruction, or caliceal/forniceal rupture [45, 46]. Urinomas typically are anechoic collections between the graft and bladder on grayscale ultrasound. Excretory phase CT/MRI can confirm urine leaks by showing extraluminal contrast (Fig. 7c). Retrograde urography and nuclear renal

scintigraphy can also detect urine extravasation but are less commonly used (Fig. 7d, e). Conservative measures like nephrostomy and stenting often resolve leaks, but severe cases may necessitate surgical interventions such as ureteral reimplantation, psoas hitch, bladder flap, or ileal conduit urinary diversion.

Perinephric abscesses often arise from graft infections or extend from abdominal wall/peritoneal infections weeks to months post-transplantation. Fever and leukocytosis with a perinephric fluid collection suggest abscess, confirmed with ultrasound showing a thick-walled, complex collection with septations, debris, and wall hypervascularity on color Doppler. Contrast-enhanced CT or MRI can assess the full extent of the collection and its impact on surrounding pelvic structures (Fig. 7f, g), possibly beyond the depth visualized by ultrasound. Like abscesses elsewhere, treatment includes systemic antibiotics and percutaneous drainage.

Lymphoceles are the most common perinephric collection, typically appearing along lymphatic pathways 2 weeks to 6 months post-transplant. They appear as thin-walled anechoic collections with internal septations on ultrasound and are usually asymptomatic but may grow enough to cause mass effect. CT shows a well-circumscribed and homogenously hypoattenuating collection, while MRI shows T1 hypointense and T2 hyperintense fluid and often thin septations within the collection.

Graft compression

Renal allograft compartment syndrome

Renal allograft compartment syndrome (RACS) is a rare but serious cause of early graft dysfunction or loss from intracompartmental hypertension in the confined iliac fossa which induces ischemia, often requiring immediate reoperation hours to days after transplant. Risk factors include extrinsic vascular compression or mismatch between donor renal size and recipient body habitus. Imaging shows edematous graft parenchyma with reduced or absent cortical flow and high-resistance waveforms, often with a perinephric hematoma (Fig. 8a, b).

Subcapsular hematoma

Subcapsular hematomas, different from perirenal hematomas, are collections of blood between the renal capsule and parenchyma, which can compress the parenchyma causing graft dysfunction and hypertension from renin release (eponymously the "Page phenomenon"), even if small. Often iatrogenic, this complication usually follows a percutaneous biopsy and presents with pain, new hypertension, graft dysfunction, and a variable hemoglobin drop. Imaging typically shows a complex, crescentic, heterogeneous collection on ultrasound and hyperdense on noncontrast CT (Fig. 8c). Spectral Doppler may show elevated resistive indices and decreased or reversed diastolic flow in otherwise normal hilar vasculature (Fig. 8d). Subcapsular hematoma with renal dysfunction or hypertension necessitates prompt surgical evacuation to save the graft.

Rejection

Graft rejection is identified and classified using the evolving Banff criteria [47], with a simpler, less specific classification—hyperacute, acute, and chronic rejection—used in clinical discussions. Hyperacute rejection, a rare event caused by pre-formed antibodies, leads to immediate microvascular occlusion and graft loss. Its imaging is non-specific and may show signs on ultrasound such as high resistance waveforms and parenchymal edema, much like with primary vascular complications. Acute rejection, typically occurring around one-week post-transplant and mediated by T-cells, also presents non-specific imaging findings such as graft edema and vascular compromise. Chronic rejection can occur over many months or years with ultrasound findings typical of chronic renal disease, such as a thinned and hyperechoic cortex.

Ultimately, the radiologist provides information for the transplant team to integrate with clinical and laboratory data to determine if abnormalities are due to rejection or a surgically intervenable cause. Histology is a valuable tool in making this determination, but the value of graft biopsy should be judiciously weighed against the risk of iatrogenic complications.

Iatrogenic complications

Intraoperative or percutaneous renal graft biopsies are common in posttransplant diagnostic workups. Standard technique uses a 16-gauge or 18-gauge biopsy device to target the renal cortex, usually the lower pole, via a cortical tangential approach to minimize injury [48]. Optimal samples contain renal cortex without medullary tissue. Major iatrogenic complications, like bleeding requiring blood transfusion or vascular embolization, are rare (0.24–4%) [45, 49–52] when performed by a subspecialized proceduralist. Less severe complications like arteriovenous fistulae and pseudoaneurysms are more common. These complications are best evaluated by ultrasound, though CTA or MRA are valuable for detailing vascular anatomy before any endovascular therapy.

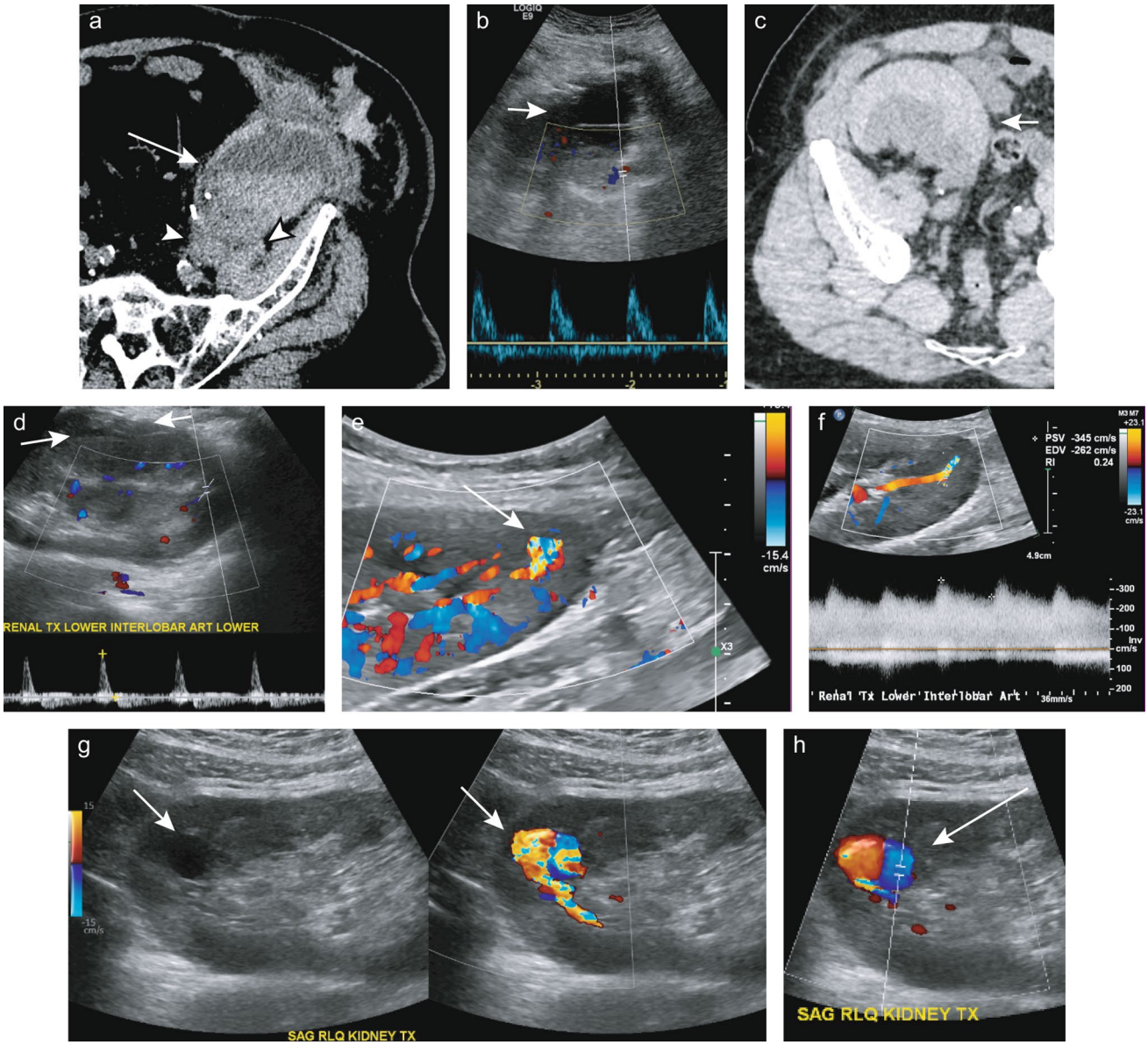

Fig. 8 Vascular injuries and consequences. **a** CT performed day-of-surgery with a large, layering hematoma (arrow) displacing and compressing the graft kidney posteriorly (arrowheads). **b** Immediately subsequent ultrasound showing the hematoma (arrow) and high resistance waveform with diastolic reversal in the renal arcuate arteries, indicating RACS. **c** Non-enhanced CT after ultrasound-guided cortical biopsy showing a crescentic, hyperattenuating collection compressing the renal cortex and effacing the sinus fat. **d** Ultrasound of the same patient showing the crescentic hematoma (arrows), sinus fat effacement, and high resistance arterial waveform with diastolic flow reversal. **e** Doppler ultrasound of a nidus of turbulent, high-velocity flow at a cortical biopsy site. **f** Doppler of an efferent vein showing high-velocity, arterialized flow of an AVF. **g** Grayscale and color Doppler ultrasound with a hypoechoic structure at a biopsy site with turbulent cortical flow and **h** a yin-yang, or Pepsi sign of a pseudoaneurysm

Iatrogenic arteriovenous fistula

Arteriovenous fistulae (AVFs) are abnormal connections between an artery and a vein, bypassing the capillary bed. This iatrogenic complication occurs in up to 15% of patients [53], is commonly asymptomatic, and may be detected incidentally on routine post-biopsy ultrasounds. Larger, clinically significant AVFs may cause hematuria, hypertension, graft dysfunction, and in severe cases, high-output heart failure. Small AVFs are commonly occult on grayscale imaging but are revealed by disorganized blood flow extending beyond normal vessel margins on color Doppler. Ultrasound may also show a feeding artery with a high-velocity, low-resistance waveform (Fig. 8e) and a vein with aliasing and arterialized waveforms (Fig. 8f). Since most iatrogenic AVFs are small, management is largely

observation and follow-up imaging, as 77% naturally regress [54]. Transcatheter embolization may be necessary for larger or symptomatic AVFs.

Iatrogenic pseudoaneurysm

Unlike AVFs, pseudoaneurysms are a contained bleed or vascular injury affecting all three layers of the artery. Iatrogenic pseudoaneurysms may be asymptomatic if small, but may cause hematuria and graft dysfunction when larger. Sonographically, small pseudoaneurysms may resemble AVFs, but larger ones appear as simple or complex cystic structures on grayscale (Fig. 8g) with to-and-fro flow and the yin-yang sign/Pepsi sign swirls on color Doppler (Fig. 8h). Pseudoaneurysm treatment varies by size; those under 2 cm are usually managed conservatively, while larger pseudoaneurysms often require transcatheter embolization [45].

Renal artery complications

Renal artery stenosis

Transplant renal artery stenosis is the most common vascular complication after kidney transplantation (1–3%) [55], typically occurring 3 months to 2 years post-transplant and presenting with refractory arterial hypertension, sometimes with declining graft function. Classic ultrasound features of transplant renal artery stenosis include focally elevated peak systolic velocity (PSV, > 340–400 cm/s) with turbulent flow aliasing at the stenosis (Fig. 9a) and main renal artery to external iliac artery PSV ratio elevation (> 1.8). Downstream

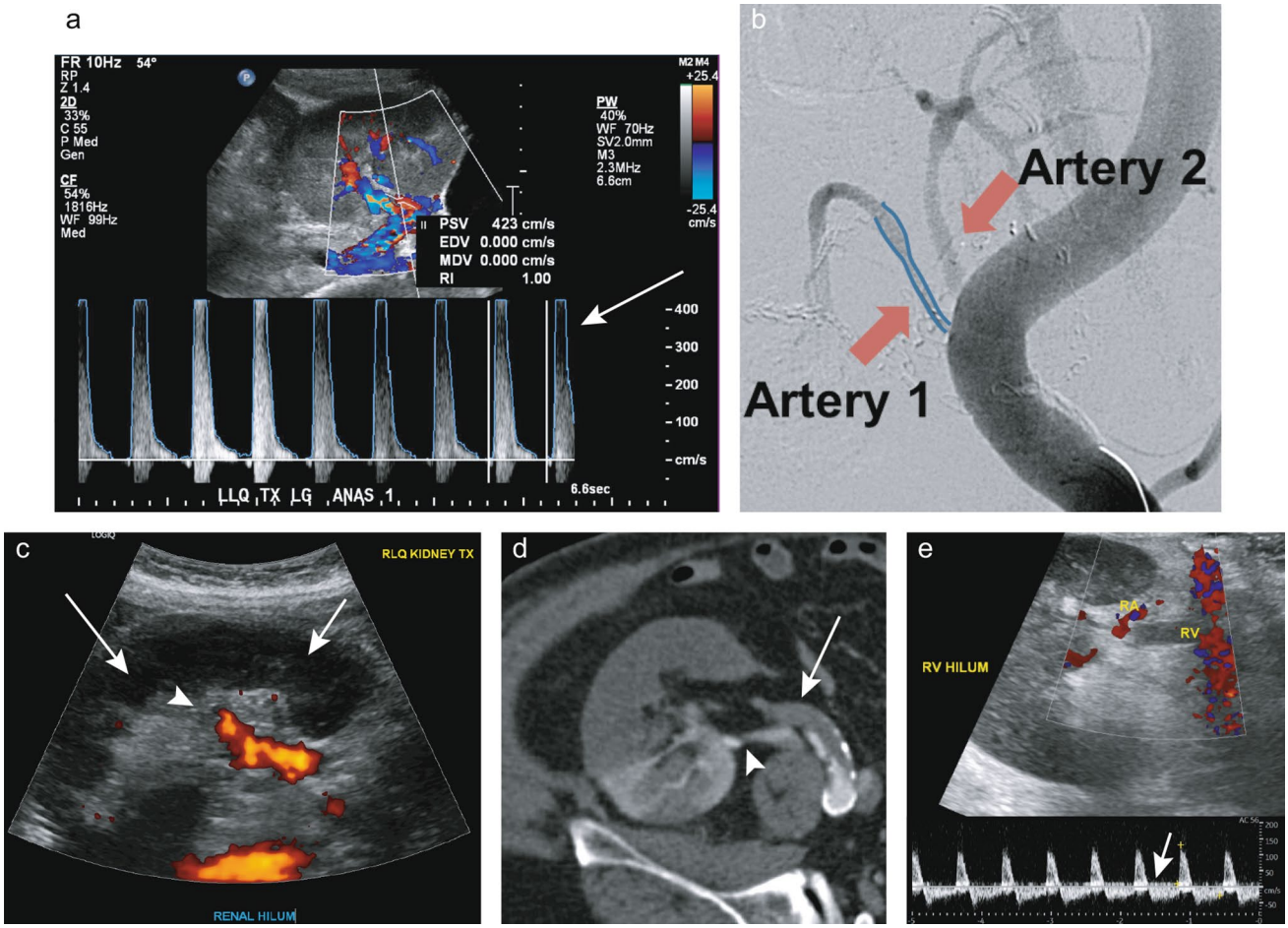

Fig. 9 Vascular compromise. **a** Elevated peak systolic velocity > 400 cm/s (arrow) with resistive index of 1.0, followed by **b** digital subtraction angiography showing stenosis of one of the paired renal arteries while artery 2 is widely patent. **c** Renal artery thrombosis with power Doppler with absent flow in the renal parenchyma (arrow) and abrupt cutoff of the renal artery and minimal arterial flow in the renal sinus (arrowhead). **d** CTA of renal artery thrombosis (arrow) with absent enhancement from the lower pole to the interpolar kidney, sparing the upper pole via a small accessory polar branch (arrowhead). **e** Renal vein thrombosis with absent flow in the vein and reversal of diastolic flow in the adjacent artery (arrow)

renal and segmental arteries often show *tardus parvus* waveforms with low RIs (< 0.50) on spectral analysis.

A common pitfall is postoperative edema at the arterial anastomosis that transiently elevates PSV, mimicking arterial stenosis. Therefore, early postoperative elevated PSV requires careful interpretation of downstream spectral waveforms and short-term follow-up ultrasound to confirm resolution. When confirmation of renal artery stenosis suspected by ultrasound is needed, options include CTA/MRA or digital subtraction angiography using iodinated contrast (Fig. 9b) or carbon dioxide. Angiography is useful diagnostically and therapeutically allowing interventions like transluminal angioplasty and stent placement. In complex or refractory cases, surgical intervention may be required to repair the stenosis.

Renal artery thrombosis

Transplant renal artery thrombosis, a rare but serious complication post-kidney transplantation (< 0.5% incidence) [56], typically occurs within hours of transplant with sudden cessation of urine output, increased hypertension, and possibly lower quadrant pain from an inflammatory reaction to the ischemic graft. Potential causes of transplant arterial thrombosis include anastomotic occlusion, hyperacute graft rejection, arterial compression or kinking, vasculitis, or an intraluminal arterial flap.

Sonographic signs of transplant renal artery thrombosis are segmental or global loss of parenchymal perfusion and absent flow in transplant renal vasculature on Doppler analysis (Fig. 9c). Rarely, ultrasound is equivocal and CTA/MRA may be used, showing nonopacification of the transplant vessels and diminished or absent contrast enhancement of the parenchyma (Fig. 9d). CTA/MRA also allows greater assessment of transplant vascular anatomy, including accessory vessels. Timely diagnosis is vital to prevent graft loss which typically requires immediate surgical reoperation.

Renal vein complications

Renal vein thrombosis

Transplant renal vein thrombosis, a major cause of early graft failure, occurs in less than 5% of adults and up to 8.2% of pediatric patients [45]. It typically develops within the first 5 days post-transplant, peaking at 48 h, presenting with sudden pain, oliguria/anuria, and possible ipsilateral lower extremity edema from thrombus propagation to the iliac veins.

Renal vein thrombosis appears as edematous or engorged renal parenchyma with lost corticomedullary differentiation on grayscale ultrasound. Typical color Doppler findings include absent flow in the vein and reversed arterial diastolic flow (Fig. 9e), however this flow reversal is nonspecific, also seen with complications including graft torsion, subcapsular hematoma compression, severe rejection, or acute tubular necrosis. Like arterial thrombosis, prompt diagnosis and treatment of renal vein thrombosis are critical for graft salvage. Acute renal vein thrombosis requires open surgical thrombectomy but still results in a high rate of graft loss. Delayed partial thrombosis may be treated with endovascular thrombolysis, albeit with a higher bleeding risk [57].

Graft tumors and mimics

Transplant recipients, due to ongoing immunosuppression, have higher risk of all malignancies, though de novo graft renal neoplasms are exceedingly rare with incidence < 0.5% [58]. Careful interpretation of transplant renal ultrasound is crucial to detect small renal neoplasms, appearing as isoechoic or hypoechoic masses with vascularity on color Doppler. CT detection can be challenging due to frequent noncontrast exams to preserve renal function (Fig. 10a); MRI is often more effective for both detection and characterization. Focal rejection, an important graft tumor mimic, may appear as a pseudomass on any modality (Fig. 10b, c).

Kidney transplant recipients are over twice as likely to be diagnosed with primary malignancies than the general population due to several factors, including oncogenic virus infections, carcinogenic medications, suppressed immune anti-tumor response, and enhanced detection from frequent imaging. The most significantly increased risks are for squamous cell carcinoma and Kaposi sarcoma, though most organs and tissues outside the brain are susceptible [59]. Post-transplant lymphoproliferative disorder (PTLD), typically associated with Epstein–Barr virus, presents with a range of imaging findings from nonspecific lymphadenopathy and masses in various tissues, including the graft (Fig. 10d) [60]. Early detection by imaging can lead to prompt immunosuppression-reduction and increased odds of response without further need for chemotherapy [61].

Future considerations

Radiologists are encountering an increasing number of kidney transplant patients, a trend that will continue as kidney transplantation follows the growing demand. Even more, we may be entering a new phase in transplant medicine highlighted by recent advancements in porcine renal xenotransplantation, with the first and second xenotransplants into humans performed at Massachusetts General Hospital and New York University, respectively [62, 63]. Momentum is building in light of new genome

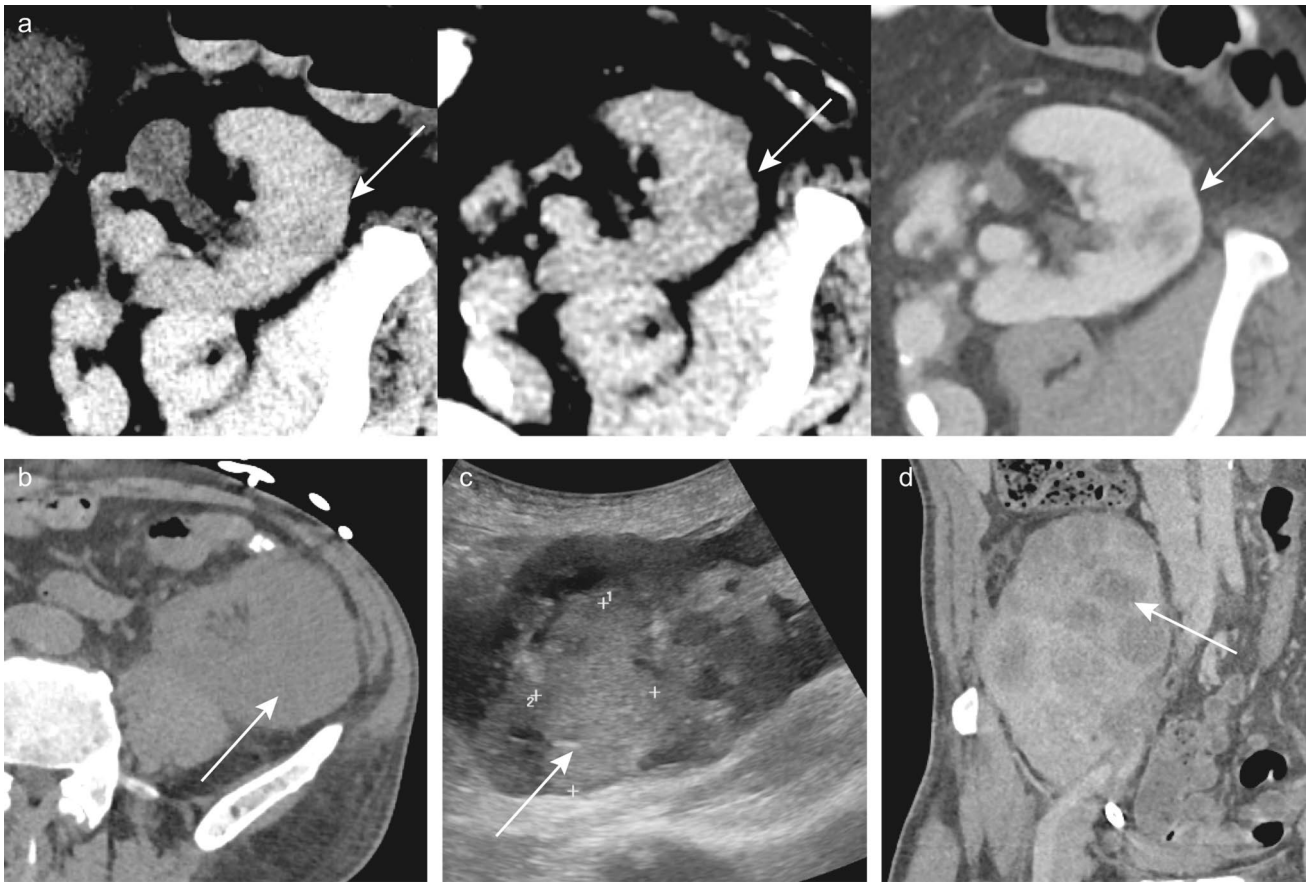

Fig. 10 Post-transplant mass lesions. **a** Growth of a solid mass in the allograft unnoticed among cysts on noncontrast CTs for two years before showing enhancement on contrast-enhanced CT. Biopsy showed oncocytoma. **b** Mass-like expansion of the graft on non-contrast CT suspicious for neoplasm, confirmed on **c** follow up ultrasound as an irregular mass. Biopsy showed focal rejection and no malignancy. **d** Post-transplant lymphoproliferative disorder (PTLD) presenting as numerous masses infiltrating the right lower quadrant renal allograft (arrow)

editing technologies [64]; xenografts will possibly provide a large source of future donor kidneys. The imaging characteristics of normal and abnormal xenografts have yet to be reported and will be one of many future research opportunities in the field.

Radiomics, advanced MRI techniques, and machine learning together are expanding the radiologist's toolkit in assessing renal graft health. Early data suggest multiple diffusion-weighted imaging parameters predict graft dysfunction independently of urine and blood chemistries, causing a push for new research in the field [65, 66]. Early reports of machine learning being used to combine clinical data with the large volume of serial imaging data are promising, further indicating the need for more research in the area [67].

Conclusions

Kidney transplantation is increasing in the United States and abroad, emphasizing the need for radiologists to know best practices of donor and post-transplant recipient evaluation. Transplant patient assessment is multidisciplinary; radiologists gain from knowing the surgical approach of donor nephrectomy and implications of post-operative complications to better communicate with referring transplant surgeons. Knowledge of the clinical manifestations of imaging findings aids radiologists in adjusting pre-test probabilities and prompting additional imaging if initial studies are inadequate. With the recent introduction of genetically

modified renal xenografts as a promising solution to the organ shortage, familiarity with transplant imaging may become further vital to the radiologist.

Declarations

Conflict of interest RJG, JD, and LAD, have no financial or other disclosures. AK- Research Grant – GE Healthcare, PanCAN, Bayer; Consultant- Bayer.

References

1. Linden PK (2009) History of Solid Organ Transplantation and Organ Donation. Critical Care Clinics 25:165–184. https://doi.org/10.1016/j.ccc.2008.12.001
2. United States Renal Data System (2023) 2023 USRDS Annual Data Report: Epidemiology of kidney disease in the United States. National Institutes of Health, National Institute of Diabetes and Digestive and Kidney Diseases, Bethesda, MD
3. Lentine KL, Smith JM, Lyden GR, Miller JM, Dolan TG, Bradbrook K, Larkin L, Temple K, Handarova DK, Weiss S, Israni AK, Snyder JJ (2024) OPTN/SRTR 2022 Annual Data Report: Kidney. Am J Transplant 24:S19–S118. https://doi.org/10.1016/j.ajt.2024.01.012
4. Sahani DV, Rastogi N, Greenfield AC, Kalva SP, Ko D, Saini S, Harris G, Mueller PR (2005) Multi-detector row CT in evaluation of 94 living renal donors by readers with varied experience. Radiology 235:905–910. https://doi.org/10.1148/radiol.2353040496
5. Sebastià C, Peri L, Salvador R, Buñesch L, Revuelta I, Alcaraz A, Nicolau C (2010) Multidetector CT of living renal donors: lessons learned from surgeons. Radiographics 30:1875–1890. https://doi.org/10.1148/rg.307105032
6. Aghayev A, Gupta S, Dabiri BE, Steigner ML (2019) Vascular imaging in renal donors. Cardiovasc Diagn Ther 9:S116–S130. https://doi.org/10.21037/cdt.2018.11.02
7. Kawamoto S, Montgomery RA, Lawler LP, Horton KM, Fishman EK (2003) Multidetector CT angiography for preoperative evaluation of living laparoscopic kidney donors. AJR Am J Roentgenol 180:1633–1638. https://doi.org/10.2214/ajr.180.6.1801633
8. Vernuccio F, Gondalia R, Churchill S, Bashir MR, Marin D (2018) CT evaluation of the renal donor and recipient. Abdom Radiol (NY) 43:2574–2588. https://doi.org/10.1007/s00261-018-1508-1
9. Toepker M, Kuehas F, Kienzl D, Herwig R, Spazierer E, Krauss B, Weber M, Seitz C, Ringl H (2014) Dual energy computerized tomography with a split bolus-a 1-stop shop for patients with suspected urinary stones? J Urol 191:792–797. https://doi.org/10.1016/j.juro.2013.10.057
10. Engelken F, Friedersdorff F, Fuller TF, Magheli A, Budde K, Halleck F, Deger S, Liefeldt L, Hamm B, Giessing M, Diederichs G (2013) Pre-operative assessment of living renal transplant donors with state-of-the-art imaging modalities: computed tomography angiography versus magnetic resonance angiography in 118 patients. World J Urol 31:983–990. https://doi.org/10.1007/s00345-012-1022-y
11. Blankholm AD, Pedersen BG, Østrat EØ, Andersen G, Stausbøl-Grøn B, Laustsen S, Ringgaard S (2015) Noncontrast-Enhanced Magnetic Resonance Versus Computed Tomography Angiography in Preoperative Evaluation of Potential Living Renal Donors. Acad Radiol 22:1368–1375. https://doi.org/10.1016/j.acra.2015.06.015
12. Li X, Xia F, Chen L, Zhang X, Mo C, Shen W (2021) One-stop preoperative assessment of renal vessels for living donors with 3.0 T non-contrast-enhanced magnetic resonance angiography: compared with computerized tomography angiography and surgical results. Br J Radiol 94:20210589. https://doi.org/10.1259/bjr.20210589
13. Guo X, Gong Y, Wu Z, Yan F, Ding X, Xu X (2020) Renal artery assessment with non-enhanced MR angiography versus digital subtraction angiography: comparison between 1.5 and 3.0 T. Eur Radiol 30:1747–1754. https://doi.org/10.1007/s00330-019-06440-0
14. George J, John GT, Oommen R, Jacob S, Jacob CK, Shastry JC (1996) Renal functional reserve in kidney donors assessed in different settings using scintigraphy. Nephron 73:154–157. https://doi.org/10.1159/000189032
15. Diez A, Powelson J, Sundaram CP, Taber TE, Mujtaba MA, Yaqub MS, Mishler DP, Goggins WC, Sharfuddin AA (2014) Correlation between CT-based measured renal volumes and nuclear-renography-based split renal function in living kidney donors. Clinical diagnostic utility and practice patterns. Clin Transplant 28:675–682. https://doi.org/10.1111/ctr.12365
16. Gaillard F, Pavlov P, Tissier A-M, Harache B, Eladari D, Timsit M-O, Fournier C, Léon C, Hignette C, Friedlander G, Correas J-M, Weinmann P, Méjean A, Houillier P, Legendre C, Courbebaisse M (2017) Use of computed tomography assessed kidney length to predict split renal GFR in living kidney donors. Eur Radiol 27:651–659. https://doi.org/10.1007/s00330-016-4410-7
17. Windisch OL, Matter M, Pascual M, Sun P, Benamran D, Bühler L, Iselin CE (2022) Robotic versus hand-assisted laparoscopic living donor nephrectomy: comparison of two minimally invasive techniques in kidney transplantation. J Robot Surg 16:1471–1481. https://doi.org/10.1007/s11701-022-01393-x
18. Xiao Q, Fu B, Song K, Chen S, Li J, Xiao J (2020) Comparison of surgical techniques in living donor nephrectomy: a systematic review and Bayesian network meta-analysis. Ann Transplant 25:e926677. https://doi.org/10.12659/AOT.926677
19. Dong J, Lu J, Zu Q, Guo G, Ma X, Li H, Yang S, Zhang X (2011) Retroperitoneal laparoscopic live-donor nephrectomy: introduction of simple hand-assisted technique (without hand port). Transplant Proc 43:1415–1417. https://doi.org/10.1016/j.transproceed.2011.02.004
20. Kang K-Y, Lee YJ, Park SC, Yang CW, Kim Y-S, Moon IS, Koh YB, Bang BK, Choi BS (2007) A comparative study of methods of estimating kidney length in kidney transplantation donors. Nephrol Dial Transplant 22:2322–2327. https://doi.org/10.1093/ndt/gfm192
21. Thakur V, Watkins T, McCarthy K, Beidl T, Underwood N, Barnes K, Cook ME (1997) Is kidney length a good predictor of kidney volume? Am J Med Sci 313:85–89. https://doi.org/10.1097/00000441-199702000-00003
22. Akoh JA, Schumacher KJ (2020) Living kidney donor assessment: Kidney length vs differential function. World J Transplant 10:173–182. https://doi.org/10.5500/wjt.v10.i6.173
23. Mitsui Y, Sadahira T, Araki M, Wada K, Tanimoto R, Ariyoshi Y, Kobayashi Y, Watanabe M, Watanabe T, Nasu Y (2018) The assessment of renal cortex and parenchymal volume using automated CT volumetry for predicting renal function after donor nephrectomy. Clin Exp Nephrol 22:453–458. https://doi.org/10.1007/s10157-017-1454-1
24. Juluru K, Rotman JA, Masi P, Spandorfer R, Ceraolo CA, Giambrone AE, Serur D, Hartono C (2015) Semiautomated CT-Based Quantification of Donor Kidney Volume Applied to a Predictive Model of Outcomes in Renal Transplantation. AJR Am J Roentgenol 204:W566-572. https://doi.org/10.2214/AJR.14.13454

25. Ebad CA, Brennan D, Chevarria J, Hussein MB, Sexton D, Mulholland D, Doyle C, O'Kelly P, Williams Y, Dunne R, O'Seaghdha C, Little D, Morrin M, Conlon PJ (2021) Is Bigger Better? Living Donor Kidney Volume as Measured by the Donor CT Angiogram in Predicting Donor and Recipient eGFR after Living Donor Kidney Transplantation. Journal of Transplantation 2021:1–6. https://doi.org/10.1155/2021/8885354
26. Mahdavi A, Negarestani AM, Masoumi N, Ansari R, Salem P, Dehesh T, Mahdavi A (2023) Studying the effect of donor kidney volume ratios to recipients' body surface area, body mass index, and total body weight on post-transplant graft function. Abdom Radiol (NY) 48:2361–2369. https://doi.org/10.1007/s00261-023-03921-1
27. Moore KL, Persaud TVN, Torchia MG (2013) The developing human: clinically oriented embryology, 9th ed. Saunders/Elsevier, Philadelphia, PA
28. Hostiuc S, Rusu MC, Negoi I, Dorobanțu B, Grigoriu M (2019) Anatomical variants of renal veins: A meta-analysis of prevalence. Sci Rep 9:10802. https://doi.org/10.1038/s41598-019-47280-8
29. Olin JW, Froehlich J, Gu X, Bacharach JM, Eagle K, Gray BH, Jaff MR, Kim ESH, Mace P, Matsumoto AH, McBane RD, Kline-Rogers E, White CJ, Gornik HL (2012) The United States Registry for Fibromuscular Dysplasia: results in the first 447 patients. Circulation 125:3182–3190. https://doi.org/10.1161/CIRCULATIONAHA.112.091223
30. Hendricks NJ, Matsumoto AH, Angle JF, Baheti A, Sabri SS, Park AW, Stone JR, Patrie JT, Dworkin L, Cooper CJ, Murphy TP, Cutlip DE (2014) Is fibromuscular dysplasia underdiagnosed? A comparison of the prevalence of FMD seen in CORAL trial participants versus a single institution population of renal donor candidates. Vasc Med 19:363–367. https://doi.org/10.1177/1358863X14544715
31. Van der Niepen P, Robberechts T, Devos H, van Tussenbroek F, Januszewicz A, Persu A (2021) Fibromuscular dysplasia: its various phenotypes in everyday practice in 2021. Kardiol Pol 79:733–744. https://doi.org/10.33963/KP.a2021.0040
32. Blondin D, Lanzman R, Schellhammer F, Oels M, Grotemeyer D, Baldus SE, Rump LC, Sandmann W, Voiculescu A (2010) Fibromuscular dysplasia in living renal donors: still a challenge to computed tomographic angiography. Eur J Radiol 75:67–71. https://doi.org/10.1016/j.ejrad.2009.03.014
33. Chen Y, Dong H, Jiang X, Zou Y-B (2022) Unifocal progressed to multifocal renal artery fibromuscular dysplasia. Eur Heart J Case Rep 6:ytab522. https://doi.org/10.1093/ehjcr/ytab522
34. Benavides CA, Csapo Z, Timmins K, Holley L, Katz SM, Van Buren CT, Kahan BD (2006) Fibromuscular dysplasia recurrence after kidney transplantation: case report. Clin Nephrol 66:67–70. https://doi.org/10.5414/cnp66067
35. Adrogue HE, Evans A, Murad DN, Nguyen H, Hebert SA, Nguyen DT, Graviss EA, Ibrahim HN (2021) Long-term outcomes of kidney donors with fibromuscular dysplasia. Nephrol Dial Transplant 36:1538–1545. https://doi.org/10.1093/ndt/gfab039
36. Arumugam S, Subbiah NK, Mariappan Senthiappan A (2020) Double Ureter: Incidence, Types, and Its Applied Significance-A Cadaveric Study. Cureus 12:e7760. https://doi.org/10.7759/cureus.7760
37. Cicek SK, Ergun S, Akıncı O, Sarıyar M (2021) Renal Vascular and Ureteral Anatomic Variations in 1859 Potential Living Renal Donors. Transplant Proc 53:2153–2156. https://doi.org/10.1016/j.transproceed.2021.07.030
38. Altinel M, Acikgoz O (2023) Standardization of Laparoscopic Donor Nephrectomy Technique in Minimizing Ureteral Complications in Renal Transplant Recipients: 10-Year Experience of a Single Center. Transplant Proc 55:1116–1120. https://doi.org/10.1016/j.transproceed.2023.02.065
39. Giessing M, Fuller F, Tuellmann M, Liefeld L, Slowinski T, Budde K, Loening SA (2008) Attitude to nephrolithiasis in the potential living kidney donor: a survey of the German kidney transplant centers and review of the literature. Clin Transplant 22:476–483. https://doi.org/10.1111/j.1399-0012.2008.00812.x
40. Rezaee-Zavareh MS, Ajudani R, Ramezani Binabaj M, Heydari F, Einollahi B (2015) Kidney Allograft Stone after Kidney Transplantation and its Association with Graft Survival. Int J Organ Transplant Med 6:114–118
41. Boyce CJ, Pickhardt PJ, Lawrence EM, Kim DH, Bruce RJ (2010) Prevalence of urolithiasis in asymptomatic adults: objective determination using low dose noncontrast computerized tomography. J Urol 183:1017–1021. https://doi.org/10.1016/j.juro.2009.11.047
42. Pushkar P, Agarwal A, Kumar S, Guleria S (2015) Endourological management of live donors with urolithiasis at the time of donor nephrectomy: a single center experience. Int Urol Nephrol 47:1123–1127. https://doi.org/10.1007/s11255-015-1007-z
43. Nicol D, Fujita S (2011) Kidneys from patients with small renal tumours used for transplantation: outcomes and results. Curr Opin Urol 21:380–385. https://doi.org/10.1097/MOU.0b013e328349638e
44. Hevia V, Hassan Zakri R, Fraser Taylor C, Bruins HM, Boissier R, Lledo E, Regele H, Budde K, Figueiredo A, Breda A, Yuan CY, Olsburgh J (2019) Effectiveness and Harms of Using Kidneys with Small Renal Tumors from Deceased or Living Donors as a Source of Renal Transplantation: A Systematic Review. Eur Urol Focus 5:508–517. https://doi.org/10.1016/j.euf.2018.01.018
45. Sugi MD, Joshi G, Maddu KK, Dahiya N, Menias CO (2019) Imaging of Renal Transplant Complications throughout the Life of the Allograft: Comprehensive Multimodality Review. RadioGraphics. https://doi.org/10.1148/rg.2019190096
46. Akbar SA, Jafri SZH, Amendola MA, Madrazo BL, Salem R, Bis KG (2005) Complications of renal transplantation. Radiographics 25:1335–1356. https://doi.org/10.1148/rg.255045133
47. Roufosse C, Simmonds N, Clahsen-van Groningen M, Haas M, Henriksen KJ, Horsfield C, Loupy A, Mengel M, Perkowska-Ptasińska A, Rabant M, Racusen LC, Solez K, Becker JU (2018) A 2018 Reference Guide to the Banff Classification of Renal Allograft Pathology. Transplantation 102:1795–1814. https://doi.org/10.1097/TP.0000000000002366
48. Patel MD, Phillips CJ, Young SW, Kriegshauser JS, Chen F, Eversman WG, Silva AC, Lorans R (2010) US-guided renal transplant biopsy: efficacy of a cortical tangential approach. Radiology 256:290–296. https://doi.org/10.1148/radiol.10091793
49. Morgan TA, Chandran S, Burger IM, Zhang CA, Goldstein RB (2016) Complications of Ultrasound-Guided Renal Transplant Biopsies. Am J Transplant 16:1298–1305. https://doi.org/10.1111/ajt.13622
50. Patel MD, Young SW, Scott Kriegshauser J, Dahiya N (2018) Ultrasound-guided renal transplant biopsy: practical and pragmatic considerations. Abdom Radiol (NY) 43:2597–2603. https://doi.org/10.1007/s00261-018-1484-5
51. Shin J, Park SY (2019) Diagnostic efficacy and safety of ultrasound-guided kidney transplant biopsy using cortex-only view: a retrospective single-center study. Eur Radiol 29:5272–5279. https://doi.org/10.1007/s00330-018-5910-4
52. Baffour FI, Hickson LJ, Stegall MD, Dean PG, Gunderson TM, Atwell TD, Kurup AN, Schmitz JJ, Park WD, Schmit GD (2017) Effects of Aspirin Therapy on Ultrasound–Guided Renal Allograft Biopsy Bleeding Complications. J Vasc Interv Radiol 28:188–194. https://doi.org/10.1016/j.jvir.2016.10.021
53. Serna-Higuita LM, Zuluaga-Quintero M, Hidalgo-Oviedo JM, Vallejo SA, Aristizabal-Alzate A, Zuluaga-Valencia GA, Nieto-Ríos JF (2021) Treatment of Post-biopsy Arteriovenous Fistula

of a Renal Graft by Selective Embolization. Indian J Nephrol 31:201–204. https://doi.org/10.4103/ijn.IJN_351_19
54. Ryuge A, Yazawa M, Kitajima K, Nakazawa R, Sasaki H, Chikaraishi T, Shibagaki Y (2018) Hemorrhagic shock due to bleeding from an arteriovenous fistula after allograft biopsy in a kidney transplant recipient: a case report. CEN Case Rep 7:5–8. https://doi.org/10.1007/s13730-017-0279-9
55. Robinson KA, Kriegshauser JS, Dahiya N, Young SW, Czaplicki CD, Patel MD (2017) Detection of transplant renal artery stenosis: determining normal velocities at the renal artery anastomosis. Abdom Radiol (NY) 42:254–259. https://doi.org/10.1007/s00261-016-0876-7
56. Ayvazoglu Soy EH, Akdur A, Kirnap M, Boyvat F, Moray G, Haberal M (2017) Vascular Complications After Renal Transplant: A Single-Center Experience. Exp Clin Transplant 15:79–83. https://doi.org/10.6002/ect.mesot2016.O65
57. Keller AK, Jorgensen TM, Jespersen B (2012) Identification of risk factors for vascular thrombosis may reduce early renal graft loss: a review of recent literature. J Transplant 2012:793461. https://doi.org/10.1155/2012/793461
58. Barama A, St-Louis G, Nicolet V, Hadjeres R, Daloze P (2005) Renal cell carcinoma in kidney allografts: a case series from a single center. Am J Transplant 5:3015–3018. https://doi.org/10.1111/j.1600-6143.2005.01099.x
59. Huo Z, Li C, Xu X, Ge F, Wang R, Wen Y, Peng H, Wu X, Liang H, Peng G, Li R, Huang D, Chen Y, Zhong R, Cheng B, Xiong S, Lin W, He J, Liang W (2020) Cancer Risks in Solid Organ Transplant Recipients: Results from a Comprehensive Analysis of 72 Cohort Studies. Oncoimmunology 9:1848068. https://doi.org/10.1080/2162402X.2020.1848068
60. Taylor AL, Marcus R, Bradley JA (2005) Post-transplant lymphoproliferative disorders (PTLD) after solid organ transplantation. Crit Rev Oncol Hematol 56:155–167. https://doi.org/10.1016/j.critrevonc.2005.03.015
61. Reshef R, Vardhanabhuti S, Luskin MR, Heitjan DF, Hadjiliadis D, Goral S, Krok KL, Goldberg LR, Porter DL, Stadtmauer EA, Tsai DE (2011) Reduction of immunosuppression as initial therapy for posttransplantation lymphoproliferative disorder(★). Am J Transplant 11:336–347. https://doi.org/10.1111/j.1600-6143.2010.03387.x
62. (2024) First gene-edited pig kidney transplant. Nat Biotechnol 42:543. https://doi.org/10.1038/s41587-024-02223-1
63. Rabin RC (2024) Grandmother Becomes Second Patient to Receive Kidney From Gene-Edited Pig. The New York Times
64. Adams AB, Blumberg EA, Gill JS, Katz E, Kawai T, Schold JD, Sykes M, Tector A, Sachs DH (2024) Enhancing Kidney Transplantation and the Role of Xenografts: Report of a Scientific Workshop Sponsored by the National Kidney Foundation. Am J Kidney Dis S0272-6386(24)00629–2. https://doi.org/10.1053/j.ajkd.2023.12.025
65. Caroli A, Schneider M, Friedli I, Ljimani A, De Seigneux S, Boor P, Gullapudi L, Kazmi I, Mendichovszky IA, Notohamiprodjo M, Selby NM, Thoeny HC, Grenier N, Vallée J-P (2018) Diffusion-weighted magnetic resonance imaging to assess diffuse renal pathology: a systematic review and statement paper. Nephrol Dial Transplant 33:ii29–ii40. https://doi.org/10.1093/ndt/gfy163
66. Wang W, Yu Y, Chen J, Zhang L, Li X (2024) Intravoxel incoherent motion diffusion-weighted imaging for predicting kidney allograft function decline: comparison with clinical parameters. Insights Imaging 15:49. https://doi.org/10.1186/s13244-024-01613-y
67. Shehata M, Shalaby A, Switala AE, El-Baz M, Ghazal M, Fraiwan L, Khalil A, El-Ghar MA, Badawy M, Bakr AM, Dwyer A, Elmaghraby A, Giridharan G, Keynton R, El-Baz A (2020) A multimodal computer-aided diagnostic system for precise identification of renal allograft rejection: Preliminary results. Med Phys 47:2427–2440. https://doi.org/10.1002/mp.14109